Southern Hemisphere Sudden Stratospheric Warmings Continue to Be Relevant Under Global Warming

Sabine Bischof[1], Pia Undine Rethmeier[1,2], Wenjuan Huo[1], Sebastian Wahl[1], and Robin Pilch Kedzierski[3]

[1]GEOMAR - Helmholtz Center for Ocean Research Kiel, Kiel, Germany
[2]Christian-Albrechts Universität Kiel, Kiel, Germany
[3]Department of Meteorology and Geophysics, Universität Wien, Vienna, Austria

Correspondence: Sabine Bischof (sbischof@geomar.de)

Abstract. In 2019, a stratospheric warming event strongly disrupted the stratospheric circulation in the Southern Hemisphere. This disruption led to negative anomalies in the Southern Annular Mode that propagated down to the troposphere and contributed to hotter and drier conditions in Australia, culminating in a devastating fire season. Although such events have been rare in the past, it remains unclear how climate change will affect their occurrence and surface impacts in the coming decades. We conducted climate model time slice experiments to investigate how frequency and associated surface responses of Southern Hemispheric stratospheric warmings change under different global warming levels (present-day, 1.5 K, 2 K, 3 K, and 4 K). Additionally, we used an ensemble of historical experiments to confirm that our model simulations accurately capture the observed response to stratospheric warmings in the Southern Hemisphere. To investigate the change in stratosphere-troposphere coupling, we distinguish between downward- and non-propagating stratospheric events based on the Southern Annular Mode response on different atmospheric levels. Our findings show that the frequency of major stratospheric warmings remains close to the historical frequency up to a warming of 2 K before decreasing more significantly. The coupling between the stratosphere and the troposphere shows a large decrease only at the 4 K warming level. Hence, as long as global warming levels remain at intermediate levels, the possibility of sudden stratospheric warmings contributing to extreme events continues to be relevant and would add to heat-related stress in Australia and Southern Africa, making adaptation to global warming more challenging.

1 Introduction

Sudden stratospheric warmings (SSWs) are extreme events in the stratosphere. They are characterized by a strong disturbance of the prevailing westerly wind regime that builds the edge of the stratospheric polar vortex. An SSW leads to a disturbance of this regime, that is characterized by an anomalous warming of the polar stratosphere in a short time. Such a warming was first discovered by Scherhag (1952) in Berlin and investigated intensively afterwards (see Baldwin et al., 2021, for a detailed overview). Labitzke (1977) categorized stratospheric warmings into different types, two of which are still frequently used: major and minor SSW events. Following the definition of the WMO (see also Charlton and Polvani, 2007; Butler et al., 2015), major SSWs are characterized by a fast and strong heating of the polar cap temperatures reversing the temperature gradient from 60°to 90°latitude and a weakening of the stratospheric polar vortex culminating in a reversal of the zonal mean zonal wind at 10 hPa and 60°latitude (U_{1060}). Minor SSWs on the other hand, only show a reversal of the temperature gradient not

of the zonal mean zonal wind. On the Northern Hemisphere (NH), major SSWs occur on average every 1.6 years, while minor SSWs are more frequent (Butler et al., 2017). SSWs are of great interest because they can have a significant impact on surface weather up to a few weeks after their onset in the stratosphere (Baldwin and Dunkerton, 2001), which is very valuable for numerical weather prediction (Sigmond et al., 2013).

While SSWs are quite frequent in the NH they are very rare in the Southern Hemisphere (SH). This difference between the hemispheres is due to differences in the mean states of the respective stratospheric polar vortices, mainly caused by a larger wave forcing in the NH (Shiotani and Hirota, 1985). To date, only one major SSW event was observed in the SH, namely in 2002 (Krüger et al., 2005; Stolarski et al., 2005). Another strong disruption of the SH polar stratosphere was observed in September 2019 (e.g., Rao et al., 2020; Safieddine et al., 2020; Wargan et al., 2020; Lim et al., 2020). It was categorized as a minor SSW, because it was not associated with a shift from westerly to easterly conditions in U_{1060}. However, it caused an anomalously small ozone hole that was comparable in size to the 2002 case (Wargan et al., 2020) and led to anomalies in the stratospheric circulation that impacted surface conditions, contributing to an extensive heat wave in Australia (Lim et al., 2021; Feng et al., 2025).

Historically and also recently other warming events that were referred to a "minor SSWs" were observed in the SH. These include the events in 1988 (Schoeberl et al., 1989; Hirota et al., 1990; Kanzawa and Kawaguchi, 1990) and 2024 (Zi et al., 2025). However, these events were much smaller in amplitude (considering polar cap temperature as well as changes in U_{1060}) as compared to the 2019 event and their definitions did not comply with the criteria for minor SSWs by the WMO (Nordström and Seppälä, 2021; Kwon et al., 2020). The relative importance of these weaker events, though, was shown in studies by Thompson et al. (2005); Lim et al. (2019); Kwon et al. (2020). These studies show that also events, that do not fall into the WMO criteria can influence Antarctic and Australian climatic conditions. The work by Kwon et al. (2020) indicates that these weak events have become more frequent in recent decades. Under strong climate change conditions (in a 4xCO2 experiment), however, the number of SH SSWs and weak vortex events was shown to decrease significantly compared to present-day conditions (Jucker et al., 2021). A comprehensive evaluation on the development of SSWs in the SH in the near future under intermediate warming conditions, though, is missing, nor has the increase in ozone been considered along with the changes in GHGs under future climate conditions. This knowledge gap leads us to our first research question, which is to understand how SSW frequency will change under different global warming levels in the SH. Another open question we want to address in this publication is how the coupling characteristics and surface imprints of these events change under global warming.

To investigate the connection between the stratosphere and the troposphere, annular modes are often considered. These are the dominant modes of stratospheric as well as tropospheric variability in the high latitudes and nicely show the connection between the two atmospheric layers. On the SH, this variability pattern is called the Southern Annular Mode (SAM, Thompson and Wallace, 2000). Strong stratospheric vortex years are connected to a positive phase of the SAM, whereas weak stratospheric vortex years are connected to a negative phase of the SAM (Thompson et al., 2005; Dennison et al., 2015; Lim et al., 2018). The coupling from the stratosphere to the troposphere is strongest in spring and summer and can lead to anomalies in the tropospheric SAM for up to 3 months after the onset of the stratospheric event (Thompson and Solomon, 2002; Thompson et al., 2005; Lim et al., 2018). The strong imprint of the stratospheric circulation anomalies in the tropospheric SAM implies

that other climatic features sensitive to the tropospheric SAM also show a strong connection to these stratospheric anomalies. The SAM can influence the position of the jet stream and storm track impacting various surface climate conditions (for a review, see Zheng et al., 2014). A negative tropospheric SAM is connected to an equatorward shift of the tropospheric jet leading to changes in other surface conditions as well, e.g., anomalous heat and a lack of precipitation over Australia, anomalous cooling and enhanced precipitation over southern South America as well as to anomalous cooling over the eastern south African region (Gillett et al., 2006; Lim et al., 2018, 2019). For positive SAM conditions, the opposite surface anomalies can be found.

In the last two decades of the 20th century, the stratospheric polar vortex was in a rather strong state caused by the depletion of stratospheric ozone due to anthropogenic emissions of chlorofluorocarbons and other halogen containing species on the one hand and by the increase in anthropogenic greenhouse gases (GHGs) on the other hand (Thompson and Solomon, 2002). More precisely, ozone depletion led to decreased absorption of solar radiation in austral spring and rising GHG levels led to enhanced longwave cooling throughout the year for example by CO_2 (Rind et al., 1990; Randel and Wu, 1999). Both processes caused a cooling and an associated strengthening of the stratospheric polar vortex. The historical period of strong ozone depletion and GHG increase was therefore connected to a positive state of the SAM that even resulted in a poleward displacement of the tropospheric jet (Thompson and Solomon, 2002; Gillett and Thompson, 2003). The tropospheric SAM trend, however, was only significant during late spring and summer, when the coupling between the stratosphere and the troposphere is the largest and ozone concentrations affect stratospheric temperatures (McLandress et al., 2010; Thompson et al., 2011).

Recently, the SH stratospheric polar vortex showed an enhanced interannual variability (Chipperfield et al., 2022). Although this variability is dynamically driven, it requires a background state which allows for upward wave propagation (Charney and Drazin, 1961). As stated above, GHGs as well as stratospheric ozone can impact the mean state of the vortex. While the observed increase in GHGs is ongoing, a leveling off in the ozone trend was observed in the beginning of the 21st century and first signs of a recovery were detected (Solomon et al., 2016). Hence, in the last two decades GHG and ozone trends did not have complementary effects on the stratospheric temperature anymore. Within this period, the two SSWs of 2002 and 2019 occurred. Both events had an impact on the surface climate that resembled characteristics of the negative phase of the tropospheric SAM (Charlton et al., 2005; Lim et al., 2021). The 2019 event contributed to the extensive heat and drought in Australia in the summer of 2019 that culminated in unprecedented wild fires in the southeast of the continent (Lim et al., 2021; Feng et al., 2025).

Under future conditions, the competing effect between ozone recovery and GHG increase on the strength of the stratospheric polar vortex will become stronger and will have a significant impact on the evolution of the SAM in the stratosphere and the troposphere during late spring and summer (Thompson and Solomon, 2005). These opposing effects and uncertainties, connected to future GHG concentrations, the rate of ozone recovery (or the onset of super recovery) and the role of the interaction between GHGs and ozone, lead to uncertainties in the mean state and the variability of the stratospheric polar vortex under future climate conditions (Hawkins and Sutton, 2009; Eyring et al., 2010; Morgenstern et al., 2014; Ivanciu et al., 2022a). This will in turn affect the probability of extreme events in the stratosphere, such as SSWs.

The knowledge we have on SH SSWs under historical atmospheric conditions in the SH is restricted to only two events that classify as SSWs under the WMO criteria (see also Supplementary Fig. S1). How frequent SH SSWs are is therefore a question

that can only roughly be estimated from observations. Considering that the data availability allows for an identification of SSWs for a maximum period of 67 years (from 1957 to 2023, Naujokat and Roscoe, 2005), a frequency of one major (minor) event per 67 (33.5) years can be estimated. Model simulations show a slightly higher frequency: Wang et al. (2020) found one major SSW every 2-3 decades in a large ensemble of the Met Office GloSea5 seasonal forecasting system, which is based on the high resolution version of the Hadley Centre Global Environment Model version 3 (HadGEM3), whereas Jucker et al. (2021) found one major (minor) SSW every 59 (22) years using a multi-millennial simulation of the Geophysical Fluid Dynamics Laboratory Coupled Model-2.1 (GFDL-CM2.1) under 1990 conditions. The estimate by Jucker et al. (2021) is very close to that estimated from observations. Under future climate conditions (4xCO2 experiment), Jucker et al. (2021) found a significant decrease in SSW occurrence: one major (minor) SSW every 883 (309) years. They attributed this strong decrease in frequency to the strengthening and to the lifetime extension of the stratospheric polar vortex. They concluded that the 2019 event might be the last one observed in this century. However, this result was based on an extreme, 4xCO2, GHG forcing setup. Changes in ozone, on the other hand, were not considered, likely resulting in an overestimation of the strengthening of the polar vortex by the end of the century. Further, climate will only see a gradual increase in GHGs as well an increase in ozone in the next decades.

The main objective of our study is to evaluate how frequency, timing and coupling characteristics of SH SSWs evolve under various intermediate and strong global warming conditions. In order to address this, we performed time slice simulations with a global atmosphere model under different global warming levels (present-day, 1.5 K, 2 K, 3 K and 4 K). To validate that the model is fit for purpose, we additionally performed an ensemble of historical simulations. The time slice simulations enable us to characterize the development of SSW occurrence for strong as well as for moderate warming levels that we might observe in the coming decades (Intergovernmental Panel on Climate Change (IPCC), 2023). To investigate changes in the surface impacts of SH SSWs we apply a method to distinguish downward propagating and non-propagating SSWs based on the definition by Karpechko et al. (2017), which was created for the NH. Here, we show that this method can also be applied for the SH. Given the large impact that the 2019 SSW had on Australian climate, it is important to close the existing knowledge gap and understand the behavior of SH SSWs under different warming levels better.

2 Data and Methods

2.1 Model Simulations

We performed model experiments with the Flexible Ocean and Climate Infrastructure, version 1 (FOCI1, Matthes et al., 2020) in the following setting: atmosphere and land model are coupled while sea surface temperatures (SSTs) and sea ice cover (SIC) are prescribed as daily mean values. FOCI1 incorporates the atmosphere model ECHAM, version 6.3.05p2, with a spectral truncation of T63 (about $\sim 1.8^\circ$ in longitude and latitude) and 95 hybrid sigma-pressure levels in the vertical with a lid at 0.01 hPa (Müller et al., 2019) enabling a realistic representation of important stratospheric features such as the quasi-biennial oscillation or the SSW frequency in the northern hemisphere (Matthes et al., 2020). It also includes the land model: Jena Scheme for Biosphere-Atmosphere Coupling in Hamburg (JSBACH), version 3 (Brovkin et al., 2009; Reick et al., 2013). In

our model settings, the dynamical vegetation is not used; vegetation and land use maps are prescribed based on CMIP6 forcing fields. This assures to have the same vegetation cover in each of the model years in the respective time slice experiments.

To analyze the effect of SH SSWs on the surface climate under different global warming levels we performed ensembles of 2 to 3 time slice experiments with about 100 years each for different global warming states: present-day, 1.5 K, 2 K, 3 K and 4 K global warming with respect to pre-industrial 2m air temperatures. All model experiments are summarized in Table 1. The time slice experiments apply perpetual atmospheric and surface conditions that follow the given global warming levels. For the present-day experiment, these conditions follow the 2018 values from the SSP5-8.5 scenario. To calculate the external forcings and boundary conditions for the other warming levels, we used a coupled FOCI1 simulation under the SSP5-8.5 scenario. The respective model years in which the individual warming levels are reached were determined, and a period of +/- 15 years for 1.5, 2 and 3 K (+/- 10 years for 4 K) was used to calculate GHG, stratospheric ozone, solar, aerosol and land use forcing conditions for the respective global warming experiments. The corresponding global mixing ratios of CO_2 are: 460.62 ppm (1.5 K), 542.21 ppm (2K), 751.62 ppm (3K) and 985.39 ppm (4K). Table 2 summarizes the GHG mixing ratios prescribed in the time slice experiments. The corresponding monthly SH ozone levels are depicted in Supplementary Figure S2.

Additionally, we performed an ensemble of 5 transient simulations under historical conditions (following CMIP6 historical forcing until 2014 and the SSP5-8.5 scenario thereafter (Meinshausen et al., 2020)) for the period of 1980 to 2019. We compare these simulations to ERA5 data (using the same 1980-2019 period), a widely used reanalysis product from the European Centre for Medium-Range Weather Forecasts (ECMWF) (Hersbach et al., 2020). For the historical, as well as for the present-day experiment, daily SSTs and SIC are prescribed based on ERA5 data: for the present-day experiment, perpetual 2018 conditions are used; for the historical experiment, transient SSTs and SIC from 1980 to 2019 are prescribed. The 2018 SST field was chosen as this year was not characterized by a specific phase of the El Niño Southern Oscillation (ENSO). To design the SST and SIC forcing for the future global warming levels, the change in SSTs from 2018 to the respective 1.5, 2, 3 and 4 K warming level periods from the coupled FOCI1 simulation was added to the daily 2018 SST field up to 60° latitude. Poleward of 60° latitude, SST and SIC smoothly transition towards the simulated SIC and SSTs from the coupled FOCI1 simulation. This ensures a daily evolution of SST and SIC in each scenario, and minimizes the impact of biases of FOCI1 equatorward of 60° latitude. For all time slice experiments, 20 days at the beginning and end of the respective forcing years were tapered for a smooth transition between the model years.

2.2 Methods

We define major and minor SSW events for the SH (all numbers are collected in Table 1). For major SSWs we follow the WMO definition for the NH (Charlton and Polvani, 2007), for which major SSW events are defined when the zonal mean zonal wind at 10 hPa and 60°N (U_{1060N}) turns easterly during winter or early spring and recovers to westerlies for at least 10 consecutive days before the end of April. For the SH event detection, we use the zonal mean zonal wind at 10 hPa and 60°S (U_{1060S}) and restrict the selection period to July to September to exclude final warmings (the transition to summer conditions). A major SSW is defined when U_{1060S} falls below 0 m/s. For minor warmings we use a threshold of 20 m/s as done in Rao et al. (2022). This method captures the observed stratospheric warmings of 2019 and 2002 in the SH when applied to ERA5

Table 1. Overview of SSW types and their frequency in ERA5 data and model experiments. In brackets the numbers of dSSWs and nSSWs are indicated (dSSWs/nSSWs). ERA5 data is restricted to the 1980 to 2019 period for comparability with the historical simulations.

Experiment	**Runs**	**Years**	**Forcing type**	All SSWs	Majors SSWs	Minor SSWs	1 SSW per	1 major SSW per
ERA5	-	40	-	2 (1/1)	1 (0/1)	1 (1/0)	20 years	40 years
historical	5	200	transient 1980 to 2019	17 (13/4)	7 (6/1)	10 (7/3)	12 years	29 years
present day	3	302	perpetual 2018 conditions	31 (26/5)	7 (7/0)	24 (19/5)	10 years	43 years
1.5K	2	203	perpetual 1.5 K warming	18 (15/3)	7 (7/0)	11 (8/3)	11 years	29 years
2K	2	204	perpetual 2 K warming	19 (10/9)	4 (4/0)	15 (6/9)	11 years	51 years
3K	2	203	perpetual 3 K warming	12 (9/3)	2 (2/0)	10 (7/3)	17 years	102 years
4K	2	201	perpetual 4 K warming	14 (9/5)	1 (1/0)	13 (8/5)	14 years	201 years

Table 2. Volume mixing ratios of well-mixed greenhouse gases prescribed in the different time slice experiments as well as SH polar cap (60-90°S) ozone at 30 hPa averaged over September and October.

Experiment	global GHG volume mixing ratios					O_3 volume mixing ratio [ppm]
	CO_2 [ppm]	CH_4 [ppb]	N_2O [ppb]	$CFC11$ [ppt]	$CFC12$ [ppt]	(60-90°S, 30 hPa, September-October)
present-day	408.76	1885.97	330.56	223.64	504.26	2.39
1.5 K	460.62	2062.88	341.68	187.94	445.14	2.75
2 K	542.21	2344.27	354.58	148.64	381.47	2.95
3 K	751.62	2639.39	373.36	96.29	294.63	3.22
4 K	985.39	2554.71	385.87	65.30	237.47	3.49

data (compare Fig. 1). The weaker events of 1988 and 2024 are not detected with this method (see Supplementary Figure S1a for an extended ERA5 period, 1950-2025). ~~Applying~~ According to the WMO definition~~for minor SSWs, which is based on the~~ , a stratospheric warming is called minor if a significant temperature increase of at least 25 K in a period of a week or less is observed at any stratospheric level in the wintertime hemisphere (Labitzke, 1981; Butler et al., 2015). Often, also the polar cap temperature gradient ~~, results in~~ is used to detect minor SSWs (Butler et al., 2017). To test how sensitive the detection of SH minor warmings is to the specific method used, we additionally show the ~~same years (Supplementary Figure S1b). Only during those two years, the~~ temperature gradient ~~between~~ from 60 ~~and~~ to 90°S ~~reverses~~ at 30 hPa in the Supplementary Figure S1b, which reverses only during 2002 and 2019 before October. We therefore consider the criterion introduced by Rao et al. (2022) to be suitable for our analysis. For large parts of the analysis we combine major and minor SSWs and refer to these as "all SSWs". We aim to investigate the average stratospheric and tropospheric response to stratospheric warmings and do therefore not discuss the synoptic patterns of individual events. We base our analysis largely on composites, for which the central date is selected to be the day on which the 20 m/s criterion is met.

Additionally, we applied a method to investigate whether an SSW signal propagates into the troposphere by distinguishing

between downward propagating and non-propagating SSWs based on the definition introduced by Karpechko et al. (2017) for the NH, that uses the Northern Annular Mode. Here, we use the Southern Annular Mode (SAM, defined below) and follow three criteria (Karpechko et al., 2017):

(1) The mean SAM index at 1000 hPa (SAM1000) over the period of 45 days (days 8-52 after day 0) must be negative

(2) the proportion of days within this 45-day period on which the daily SAM1000 is negative shall be at least 50%

(3) the proportion of days within that 45-day period on which the daily SAM indices in the lower stratosphere (SAM150) are negative shall be at least 70%

The number of downward propagating events (dSSWs) and non-propagating events (nSSWs) are shown in Table 1 for each experiment.

The SAM is defined analogous to a simple approach used for the Northern Annular Mode in Karpechko et al. (2017): geopotential height (GPH) is averaged over the polar cap (60-90°S) after the values are area-weighted. The daily climatology is subtracted to calculate the respective anomalies for each pressure level. After that, the data in each level are normalized by its standard deviation. Conventionally, the SAM is defined as negative if the polar cap GPH anomalies are positive. To achieve this, the SAM index is multiplied by minus 1 for each pressure level.

For the surface responses to SSWs as well as for the SSW downward propagation signal in the SAM, composite analysis is applied. For the SAM, composites are calculated with respect to the central day of the SSW events. For the surface response, the anomaly of the October to December period for SSW years is used, which is similar to the definition used in Lim et al. (2019), who considered the period of October to January in their analyses. Significant differences of these composites to the mean state are calculated based on a two-sided t-test when applicable. The October-November-December mean state is included in the Supplement (Supplementary Figure S3). Statistical significance is indicated for p-values ≤ 0.05.

3 Results: SSWs in FOCI1 and its effect on Australian heat events

3.1 SH SSWs under historical and present-day conditions

Before we investigate the impact of climate change on the frequency and surface impacts of stratospheric warmings, we want to show how well FOCI1 represents SH SSWs and their impact onto the surface under historical and present-day conditions. Figure 1 shows the zonal mean zonal wind at 10 hPa and 60°S for the historical ensemble (Fig. 1a) and for ERA5 (Fig. 1b), both representing the same period of 1980 to 2019. For the model results an ensemble of 5 realizations is shown (Table 1). The multiyear mean (thick gray line) shows that the maximum wind in FOCI1 is reached earlier than in ERA5 but that it is of comparable magnitude. In contrast to the reanalysis data, our historical ensemble shows a larger spread among modeled years, reflecting a higher interannual variability in the strength of the polar vortex in comparison to ERA5. The colored lines show those years that classify as years with a minor or major warming according to the definitions for major and minor warmings

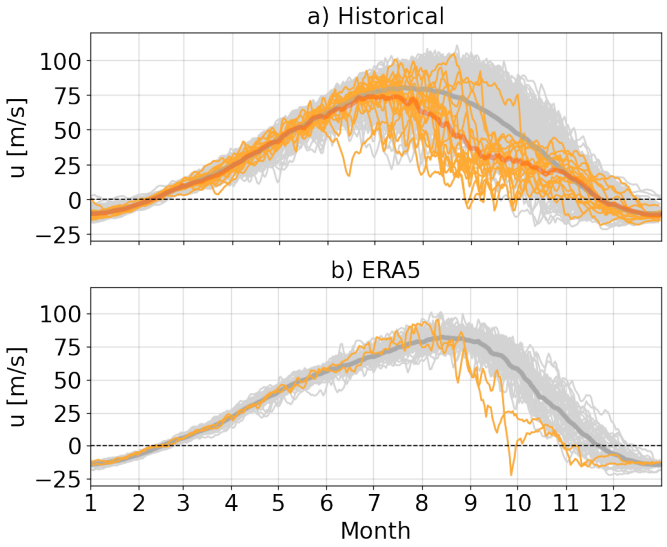

Figure 1. Annual cycle of zonal mean zonal wind (U) at 10 hPa and 60°S of individual years (thin gray lines) and the multi-year mean (thick gray line) for a) the historical model ensemble and b) ERA5 data. Both data sets covering the same period of 1980-2019. Thin orange lines indicate years for which a stratospheric warming event was found. The thick orange line shows the mean of all SSW years. The dashed line highlights the zero wind line. The ticks on the x-axis indicate the start of the months.

given above. The observed warming years, 2002 and 2019, are clearly captured in ERA5 (Fig. 1b). Comparing Figures 1a and b shows that SSWs occur earlier and that the frequency of SSWs is likely overestimated in our model simulations; in the historical ensemble it is almost twice as high as in ERA5 (see Table 1). However, the occurrence of SSWs for single ensemble members ranges from 0 to 7 events in the 40-year period from 1980 to 2019. The number of observed SSWs falls within this spread. Nevertheless, the variability in the strength of the polar stratospheric vortex is larger in our model compared to observations, which probably leads to a higher frequency in SSWs. For our study, this likely overestimation of stratospheric warming events is not considered problematic, since we do not claim to predict the frequency of SSWs in the future. We rather aim on investigating how much the SSW frequency and their surface impacts can change in comparison to recent climate conditions. In previous studies, FOCI1 was shown to capture SH stratospheric dynamics very well (Ivanciu et al., 2021, 2022a, b; Xu et al., 2025). Also the NH SSW frequency was evaluated (Matthes et al., 2020): it is with 0.44 events per year close to reanalysis (0.52 events per year) and lies well within the CMIP6 model spread shown in Wu and Reichler (2020).

To evaluate FOCI's representation of the impact of SH SSWs on the troposphere, we will focus on the SSW related anomalies of the SAM next. The temporal evolution of SAM anomalies throughout the middle and lower atmosphere following the defined SSW events is depicted in Figure 2a. Minor and major warmings are considered together in this figure. The central day is defined as the first day for which U_{1060S} drops below 20 m/s for major and minor warmings. The negative stratospheric SAM anomaly associated with an SSW event sets in already before the criterion for the SSW is met. It propagates downward within the stratosphere after the central day and persists in a large region of the lower stratosphere for up to 60 days after the

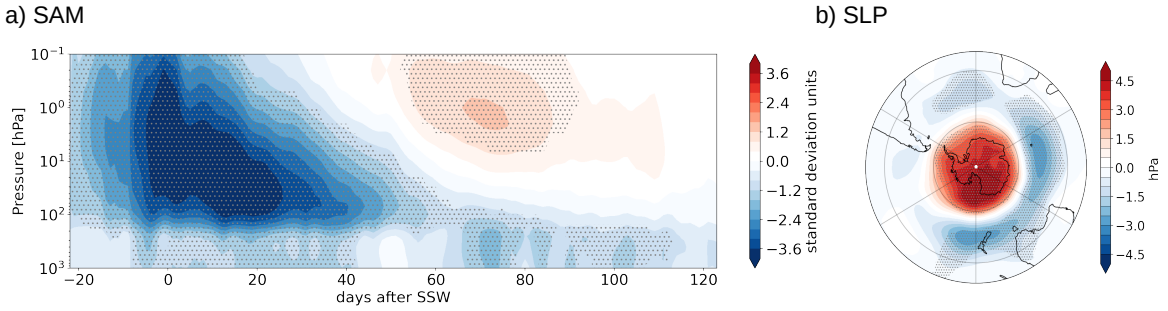

Figure 2. SSW composites for the historical model ensemble of a) Southern Annular Mode (SAM) anomalies relative to the central day (day 0) and of (b) SLP anomalies averaged over October, November and December in SSW years / following an SSW. The numbers of events included in the composite analysis are given in Table 1. Areas that show significant anomalies with respect to the climatology based on a two-sided t-test are stippled (p-value ≤ 0.05).

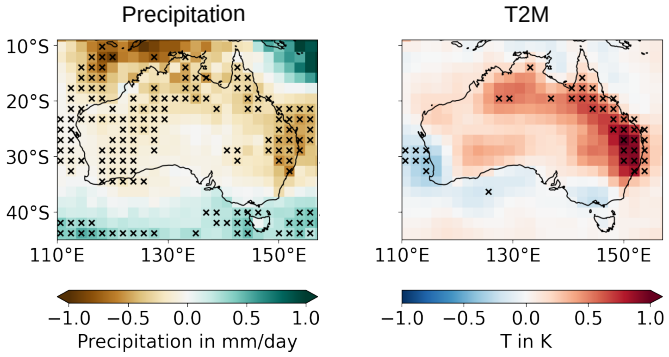

Figure 3. SSW composite for the historical model ensemble of anomalies in precipitation (left) and 2m air temperature (right). Anomalies are averaged over the October-November-December period for years with an SSW. The numbers of events included in the composite analysis are given in Table 1. Significance with respect to the climatology is indicated by stippling ($p - value \leq 0.05$).

SSW onset. The tropospheric SAM is negative from about 5 days before the central day and stays negative for more than 100 days. This persistent SAM anomaly has influences onto the surface climate. Figure 2b shows the SLP anomaly during SSW summers. It shows a clear annular mode signature with high pressure anomalies over Antarctica and a low pressure anomaly band between 30 to 50°S. However, the low SLP anomaly band is not completely symmetric around the pole. Largest anomalies are found in the Indian and West-Pacific sectors of the Southern Ocean, impacting especially the Australian continent where we find significant anomalies in precipitation and 2m air temperature (T2M) during SSW summers (Fig. 3). These are dominated by precipitation deficiencies over large parts of Australia and enhanced air temperatures over the north-eastern part of the country. This response compares very well to the findings by Lim et al. (2019) and Lim et al. (2021).

In order to address the evolution of SSWs under global warming conditions, time slice experiments under different global warming levels were conducted. To ensure that this model setup compares well to the historical ensemble run under transient

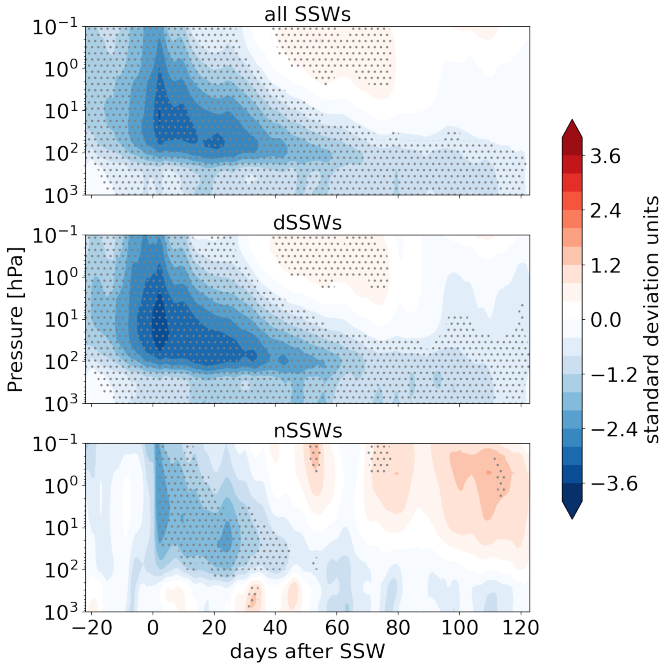

Figure 4. Composite of Southern Annular Mode anomalies relative to the central day (day 0) of different SSW events for the present-day model experiment: (top to bottom) all SSWs, downward propagating SSWs (dSSWs) and non-propagating SSWs (nSSWs). The numbers of events included in the composite analysis are given in Table 1. Areas that show significant SAM anomalies with respect to the climatology based on a two-sided t-test are stippled (p-value ≤ 0.05).

conditions, we ran a time-slice simulation under present-day (perpetual 2018) conditions, which we want to consider first. Table 1 shows that the frequency of SSWs in this experimental setup is close to the historical ensemble (1 SSW every 12 years and every 10 years respectively). The downward propagation of the SAM anomalies (Fig. 4a), as well as the surface response in SLP (Fig. 5a), temperature and precipitation (Fig. 6a) compare very well to our results from the historical ensemble. The largest difference in the response is found in western Australia, where the present-day experiment lacks the deficit in precipitation but shows a significant increase in air temperature in comparison to the historical ensemble. However, with these differences, the response of the present-day experiment fits the observed response as described by Lim et al. (2019) even better than our historical setup did. We will therefore use this time slice setup for further analyses.

3.2 Downward coupling of SH SSWs

To test how stratosphere-troposphere coupling changes under global warming, we distinguish between downward propagating SSWs (dSSWs) and non-propagating SSWs (nSSWs). The numbers of dSSWs and nSSWs in the different experiments are shown in Table 1 in brackets. While almost all major warmings classify as dSSWs, minor warmings can classify as both types.

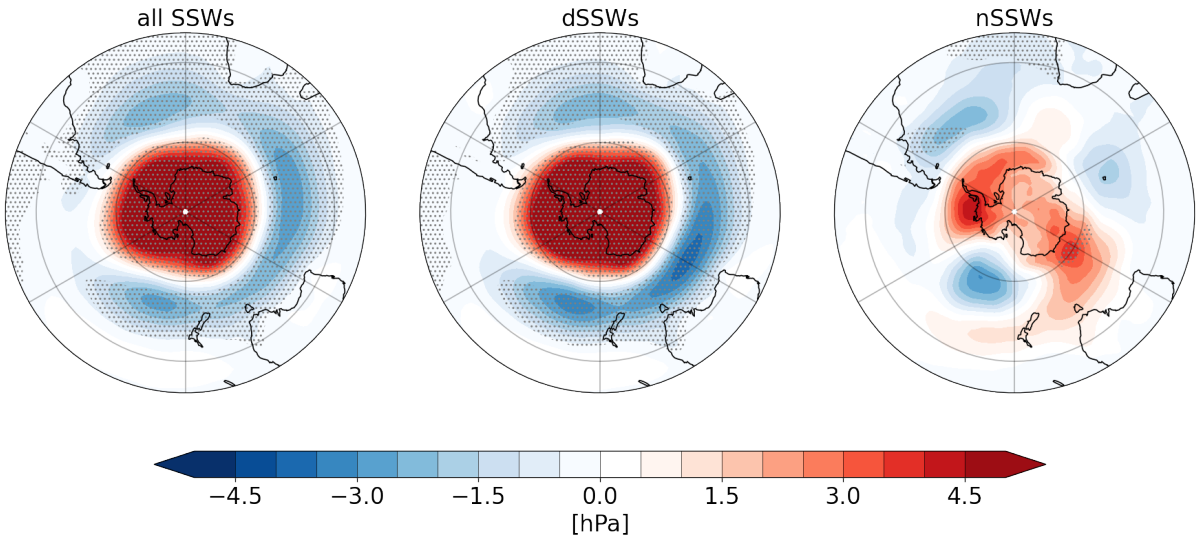

Figure 5. Composite of SLP anomalies for the present-day model experiment averaged over OND for (left to right) years with SSWs, years with downward propagating SSWs (dSSWs) and years with non-propagating SSWs (nSSWs). The numbers of events included in the composite analysis are given in Table 1. Stippling indicates significance (p-value ≤ 0.05)

Table 3. Number of dSSWs and nSSWs per decade under different global warming levels.

Experiment	dSSWs/decade	nSSWs/decade
historical	0.65	0.20
present day	0.86	0.17
1.5K	0.74	0.15
2K	0.49	0.44
3K	0.44	0.15
4K	0.45	0.25

The atmospheric responses to dSSW and nSSW events for the present-day experiment are shown in Figures 4-6b and 4-6c, respectively. It becomes clear that the method, which was introduced by Karpechko et al. (2017) for the NH, also fits very well for the SH. In winters with dSSWs a clear negative SAM-like response is found in the atmosphere. Further, dSSWs dominate the composites when considering all SSWs. The tropospheric SAM does not show any significant negative anomalies after
250 nSSWs (Fig. 4c), which is in line with the surface SLP response to nSSWs missing the typical annular mode like structure (Fig. 5c) and with the missing surface response in temperature and precipitation over the Australian continent (Fig. 6c). The lack of negative SAM anomalies during nSSWs as well as the insignificant surface responses imply that the stratosphere does not influence the troposphere after nSSWs. Hence, the comparison between dSSW and nSSW occurrence shall give valuable information on the strength of the stratosphere-troposphere coupling between the different simulations.

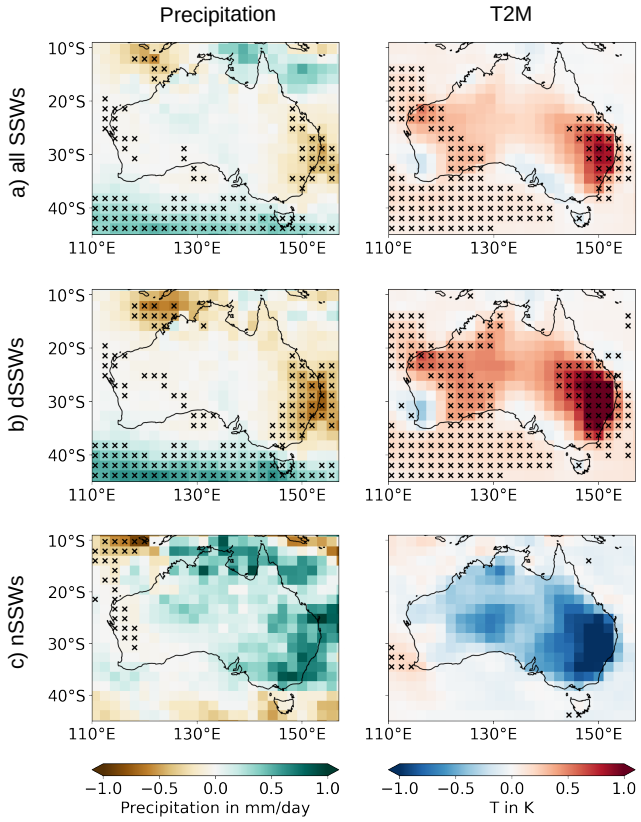

Figure 6. SSW composite for the present-day model experiment of anomalies in precipitation (left) and 2m air temperature (right) for a) all SSWs, b) downward propagating SSWs (dSSWs) and c) non-propagating SSWs (nSSWs). Anomalies are averaged over the October-November-December period for years with respective SSW events. The numbers of events included in the composite analysis are given in Table 1. Significance is indicated by stippling ($p - value \leq 0.05$).

Table 3 shows the frequency of dSSWs and nSSWs per decade for all the model experiments we conducted. Comparing the historical to the present-day experiments shows that dSSWs are more frequent under present-day conditions (0.65 dSSw/decade vs. 0.86 dSSWs/decade), while the frequency of nSSWs is very similar between both experiments (0.20 nSSWs/decade vs. 0.17 nSSWs/decade).

3.3 Global warming conditions

Under global warming conditions, our experiments show a decrease in the frequency of dSSWs from 0.65-0.86 dSSW/decade under historical and present-day conditions to about 0.45 dSSWs/decade for a warming of 3 to 4 K (Table 3). The frequency of nSSWs does not decrease linearly with global warming; it stays between 0.15 and 0.25 nSSWs/decade, with the exception of the 2 K experiment, in which we find a higher frequency of nSSWs (0.44 nSSWs/decade). Overall, the ratio between

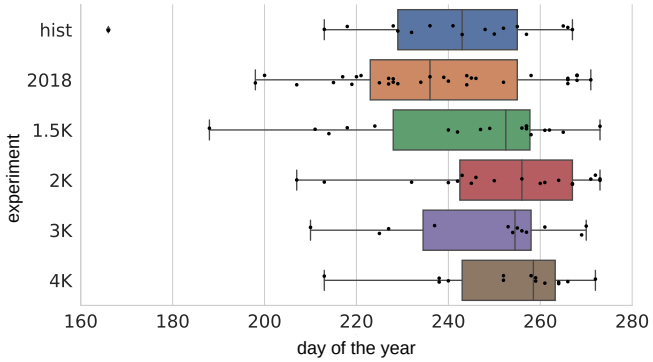

Figure 7. Boxplot of SSW onset days ($U_{1060S} < 20m/s$). Different colors denote the different model experiments. Black dots show the individual events that were considered for the statistics, while diamonds show outliers. The box represents the quartiles, the whiskers the spread of the distribution (excluding outliers). The median is indicated by a solid line. The exact number of events per experiment can be found in Table 1. For comparison, the onset days for the observed 2002 event would be day 266, for the 2019 event it would be day 259 based on ERA5 data.

dSSWs and nSSWs indicates that the coupling between the stratosphere and the troposphere decreases under increasing levels of global warming, although not linearly. This non-linearity might be due the interplay between ozone recovery and GHG increase, which will be discussed later.

Figure 7 shows the distribution of SSW onset days among the different experiments. While the median of the distribution is close to day 240 for the historical and the present-day experiments, it shifts towards later onset dates starting already at a warming of 1.5K. Late warmings are frequent especially for the 2K warming experiment. Distinguishing between dSSW and nSSW onset days indicates that dSSWs tend to occur earlier in the season than nSSWs in the time slice experiments under present-day, 1.5K and 2K conditions (Supplementary Fig. S4). This relation, however, might be influenced by the small number of nSSWs in comparison to dSSWs and should be interpreted with caution.

The decrease in dSSWs with global warming (Table 3) generally leads to a decrease in the strength of the coupling between the stratosphere and the troposphere. This response is not linearly reflected in the SAM and surface anomalies (Fig. 8). While the number of nSSWs is very high in the 2K experiment, the downward propagating events are exceptionally strong and long-lasting and dominate the composites with strong signals in precipitation and temperature anomalies over Australia (Supplementary Figs. S5 and S6). On the other hand, for the 1.5K warming ensemble, the surface response is relatively weak compared to the historical, present-day, 2K and 3K warming experiments (compare Figs. 3, 6, and 8).

A clear cut in the SAM and surface responses to SSWs occurs only under 4K conditions. In this experiment the SLP response is insignificant and also the precipitation and temperature signals over Australia differ remarkably from the response under present-day and historical conditions (Fig. 8, bottom row corresponding to 4 K warming level). However, when considering only dSSWs (Supplementary Fig. S5) the typical precipitation response over eastern Australia is also apparent for a 4K warmer world, the T2M response stays insignificant.

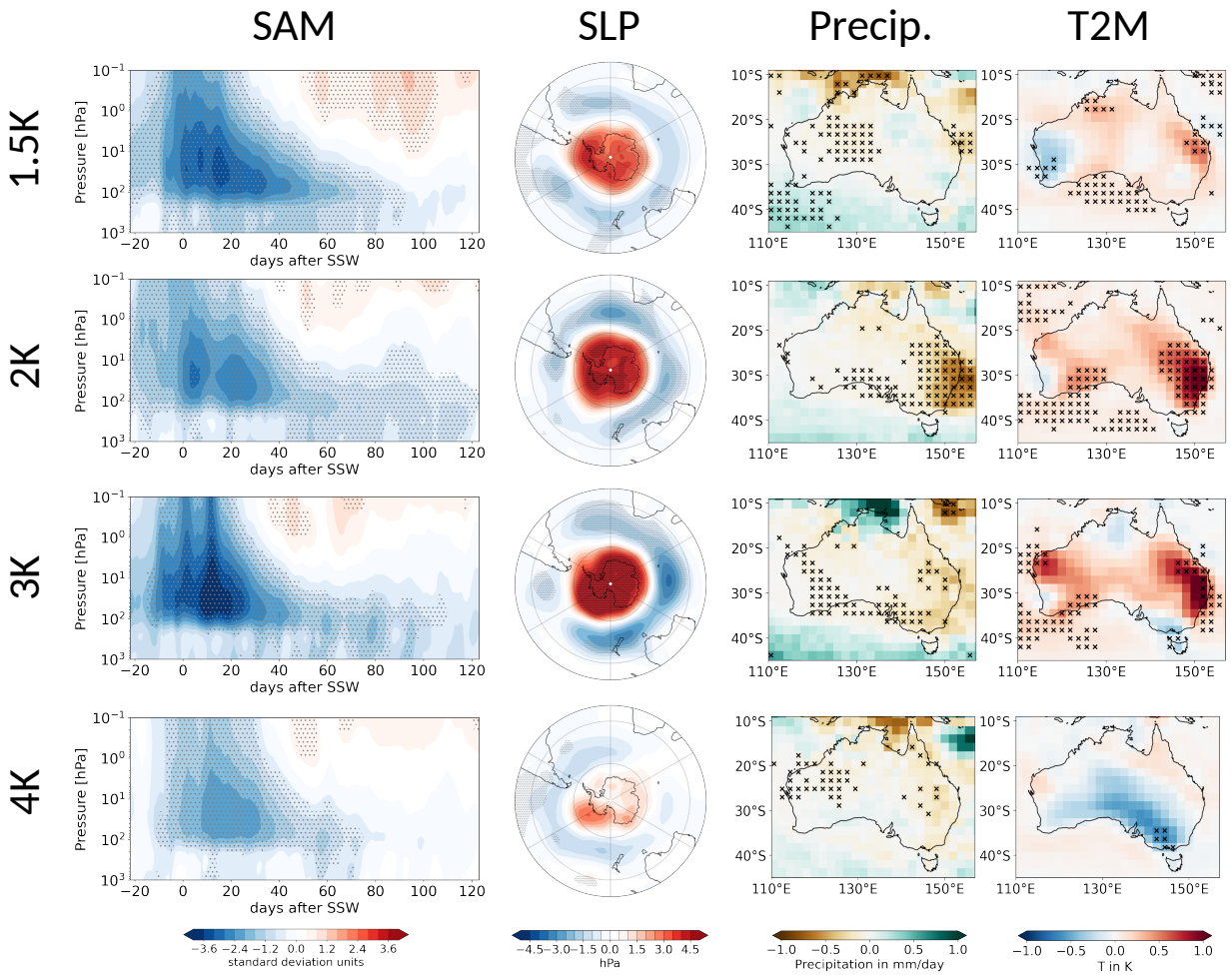

Figure 8. SSW composites for the different global warming model experiments: 1.5 K, 2 K, 3 K, and 4 K (top to bottom) showing anomalies of the SAM with respect to the central day of the SSWs, as well as of SLP, precipitation (Precip.) and 2 m air temperature (T2M) averaged over OND for years with SSWs (left to right). The numbers of events included in the composite analysis are given in Table 1. Stippling indicates statistical significance ($p - value \leq 0.05$).

The hemisphere-wide SLP response to SSWs implies that also other regions on the SH, might be affected by changes in the mean circulation, i.e., jet position. Another region that we find to be significantly impacted by SH SSWs in our model simulations is south Africa. Figure 9 shows the surface response to SSWs in precipitation and T2M over the southern tip of the African continent for all of the model experiments. Under historical and present-day conditions, the temperature response shows a tendency for warmer than normal conditions in the south east of the continent. However, this signal is only marginally significant. The precipitation response, which can be described by drier than normal conditions, dominates over Mozambique and Madagascar for the historical ensemble and over the country of South Africa in the present-day simulation. A similar

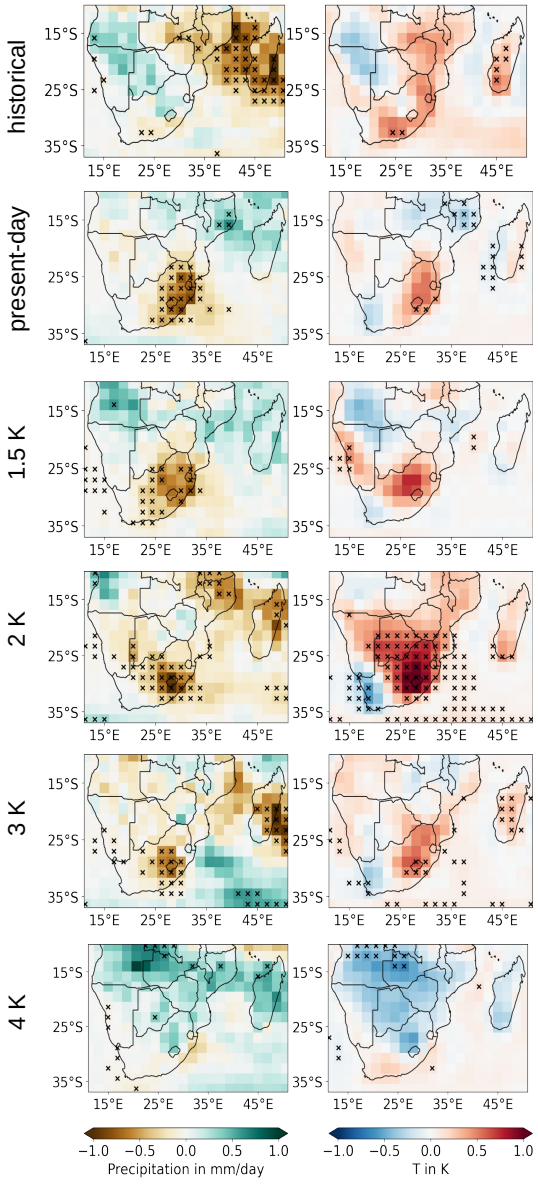

Figure 9. SSW composites for South Africa in all model experiments: historical, present-day, 1.5K, 2K, 3K, and 4K (top to bottom) showing anomalies in precipitation (left column) and 2 m air temperature (right column) averaged over OND for years with SSWs. The numbers of events included in the composite analysis are given in Table 1. Stippling indicates statistical significance ($p - value \leq 0.05$).

behavior in temperature and precipitation was found by (Lim et al., 2021) following the 2019 minor SSW event. Gillett et al. (2006), who regressed the SAM index onto station measurements of T2M and precipitation, also found a significant precipitation deficit in south Africa for negative SAM conditions, while not detecting a significant temperature response in that region.

The global warming time slice experiments agree on the deficit in precipitation over this southern most region of the African continent up to a warming of 3 K. The temperature response is of less statistical significance with the exception of the 2K experiment, which also showed the strongest surface response over Australia (Fig. 8). For a warming of 4 K, no significant response to SSWs can be found over south Africa. This is in agreement with the previously described reduction in STC in this experiment. These surface responses to SSWs over the south African continent are consistent with the response to dSSWs only (Supplementary Fig. S7).

We do not find such a robust SSW response in precipitation and air temperature over New Zealand and South America among the different experiments (Supplementary Figs. S8 and S9). However, our simulations are indicative of a tendency for wetter and colder conditions over southern South America and New Zealand after SH SSWs, which is in line with the general SAM response presented in Gillett et al. (2006).

3.4 Effect of ozone recovery

To analyze why the SSW frequency changes with global warming, we consider the change in the zonal mean zonal wind at 10 hPa between 55 to 65°S and the polar cap temperature (south of 60°S) at 30 hPa (Fig. 10). Figures 10a and b show the climatologies for the different time slice experiments, while Fig. 10c and d show the differences of the warming experiments to the present-day experiment (blue line). As expected, the lower stratosphere gets colder throughout the year under increasing levels of global warming, i.e. increasing GHG levels (Table 2). This also leads to an increase in strength of the stratospheric polar vortex throughout most of its lifetime. These changes, however, are not only dependent on the GHG concentrations that drive the level of global warming, but also on the recovery of ozone (Supplementary Fig. S2), whose effect is most pronounced in austral spring. In fact, most of the global warming experiments show a decrease in the strength of the westerly winds between 55 to 65°S at 10 hPa during that time of the year (between days 270 and 340). The change in the strength of the westerly wind with respect to the present-day experiment is remarkably similar for the warming levels of 1.5, 2 and 3 K during this time of year. Also the 4K experiment shows this weakening of the westerly winds later in the year, i.e. at the end of the polar vortex lifetime. Ozone recovery therefore leads to a weakening of the stratospheric polar vortex during spring time, the time of the year that is most important for the development of SSWs.

Considering the temperature response, all but the 4K experiment show polar cap temperatures that are similar to present-day conditions or higher in spring peaking around day 300. This indicates that the interplay between GHG increase and ozone recovery plays a key role in the strength of the vortex (in agreement with McLandress et al., 2010). It is the period between days 250 and 260 (beginning of September) in which most of the SSWs occur in the global warming experiments (Fig. 7). This is the period, when zonal winds are closest to the present-day conditions in the 1.5, 2 and 3K global warming experiments (Fig. 10). The 4K experiment is the only one that does not reach present-day levels in polar cap temperature in spring. The associated strengthening of the polar stratospheric vortex diminishes wave propagation (Charney and Drazin, 1961) and decreases the likelihood of SSWs. The missing surface response to SSWs under 4 K warming conditions is not as easily attributable to the interplay between GHGs and stratospheric ozone and further analysis would be needed to understand the underlying reasons

for this apparent decrease in STC under large global warming levels.

This interplay between GHG increase and ozone recovery might be responsible for the non-linear response that we found in our time slice experiments (Table 3 and Figure 8). However, why exactly the 2 K experiment behaves so differently compared to the other warming experiments remains unclear. As described above, in the 2 K experiment a relatively larger number of nSSWs is found. The composite of these events show significant surface anomalies although the downward connection of the events is not significant. This, however, seems not to be directly connected to the ozone recovery effect onto the polar cap temperatures, since the mean polar cap temperatures during spring are very close to those in the present-day experiment (Fig. 10).

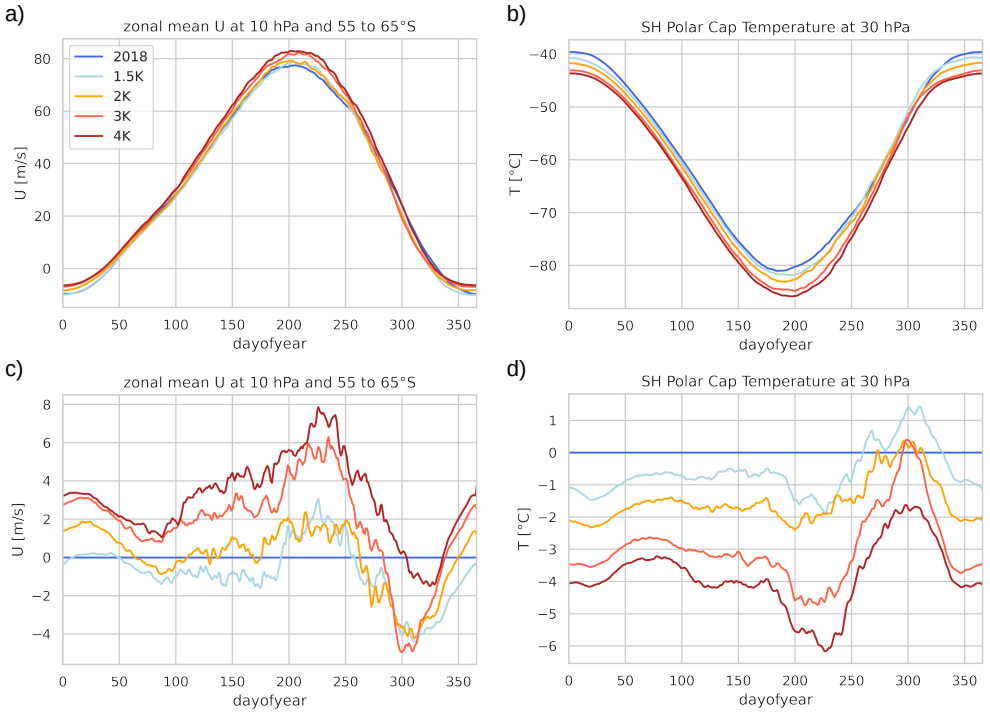

Figure 10. Seasonal cycle of zonal mean zonal wind at 10 hPa and 55 to 65°S (a) and polar cap temperatures at 30 hPa (b) for the different time slice experiments: 2018 (present-day, dark blue), 1.5 K (light blue), 2K (yellow), 3K (orange), and 4K (red). (c) and (d) as in (a) and (b) but as the anomaly between the different global warming experiments to the present-day experiment.

4 Conclusion

In this paper we investigated the frequency of SH SSWs, the change in coupling strength between the stratosphere and troposphere for these events under different global warming levels (present-day, 1.5 K, 2 K, 3 K and 4 K) and the associated changes in surface responses to SH SSWs.

Our FOCI1 experiments simulate the expected response to SSWs over Australia as presented in Lim et al. (2019) under historical and present-day conditions with positive temperature and negative precipitation anomalies during summer over eastern Australia in SSW years (see section 3.1). We found that this response is also expected for global warming levels of up to 3 K, while no significant surface response was found for a warming of 4 K.

As expected, we find a decrease in the frequency of SSWs under global warming. The strongest decrease is found for the number of major SSWs from about 1 major SSW in 30 to 40 years under present-day conditions to 1 major SSW in 200 years under a global warming of 4 K. Considering downward propagating SSWs (dSSWs), we find a decrease from 0.65-0.86 dSSW/decade under historical and present-day conditions to about 0.45 dSSWs/decade for the warming levels of 3 to 4 K (Tables 1 and 3).

With these results we add on to the study by Jucker et al. (2021), who investigate how likely SH SSWs will be under an end-of-the-century increase in atmospheric CO_2 concentrations in comparison to a perpetual 1990 simulation. They found that SH SSWs will be very unlikely under these extreme future CO_2 concentrations, due to an intensification of the stratospheric polar vortex that would further decrease the ability of vertical wave propagation and therefore the disturbance of the vortex itself. Including intermediate warming levels, we find that a remarkable decrease in SSW frequency and their surface impacts will only become likely under a global warming level of 4 K. A few differences to the study by Jucker et al. (2021) should be highlighted: In comparison to the study by Jucker et al. (2021) the frequency of SSWs is higher in our FOCI1 simulations under present-day conditions: 1 SSW every 10 years in our simulation and 1 SSW every 22 years in Jucker et al. (2021). Furthermore, while Jucker et al. (2021) find a strong decrease in SSW frequency under high GHG forcing (1 event every 309 years), the frequency in our simulations decreases only slightly (to 1 event every 14 to 17 years, see Table 1). This difference can at least partly be attributed to a different experimental design. In contrast to Jucker et al. (2021) we prescribe SSTs and SICs and their absolute difference in CO_2 concentrations is overall larger than in our present-day vs. 4K experiment. More importantly though, we consider a stratospheric ozone recovery together with the GHG increase (Table 2, Supplementary Figure S2). This counteracts the strengthening of the polar stratospheric vortex caused by increasing GHG levels, especially in the spring season, leading to even weaker than present-day zonal mean zonal wind conditions at 10 hPa between 55 to 65°S (Fig. 10).

Here, we showed that the timing of a decrease in SSW frequency depends on the interplay between GHG increase and ozone recovery. Ozone recovery is of particular importance since it is of largest amplitude in September when most SSWs occur. We found a non-linear response in SSW frequency and surface response to global warming level, which is probably due to the level of ozone recovery at the different warming levels. We found a strong surface response at the 2 K warming level, which is not clearly attributable to the specific forcing. We are not sure why this experiment stands out; one hint might be the rather late onset of the SSWs under 2 K warming. Other aspects, as for example the quasi-biennial oscillation, which is internally generated in our model, might also contribute to the non-linearity. ENSO, on the other hand, should not play a role since there is no interannual variability within the specific time slice experiments, nor are the SST warming patterns characterized by strong ENSO signals (not shown). Nevertheless, our findings imply that the strength of the polar stratospheric vortex will allow for the occurrence of SSWs on the SH under climate change conditions due to ozone recovery that is counteracting the ongoing

increase in GHG concentrations and the associated cooling of the stratosphere.

Given that the CMIP6 ozone recovery used in our study is weaker than in interactive chemistry climate models (CCMs) (Ivanciu et al., 2022b; Revell et al., 2022), the actual impact of ozone recovery might be even larger than suggested by our simulations. Another aspect that might further enhance the impact of ozone on the occurrence of SSWs are positive feedbacks between stratospheric ozone and stratospheric dynamics (Haase et al., 2020). The general importance of the ozone forcing for SH SSWs was shown in different studies: In the medium-range ECMWF forecasting system, improvements in the response of high-latitude tropospheric winds to the 2002 SSW event were found when including a new stratospheric ozone model, which significantly improved the representation of the SH stratospheric polar vortex including it's seasonality (Monge-Sanz et al., 2022). Particularly, for the 2002 major SSW, Hendon et al. (2020) showed that the stratospheric SAM anomaly and the associated surface responses over Australia connected to this warming were enhanced by positive ozone feedbacks. These interactions are only represented in interactive CCMs.

Despite missing chemistry-climate feedbacks in our model setup, the prescribed recovery of the ozone layer counteracts the GHG-driven strengthening of the polar stratospheric vortex in such a way that the frequency of SSWs remains nearly unchanged up to a warming of 2 K. This suggests that SH SSWs and their impacts on weather conditions in Australia and southern Africa, as shown in Figures 8 and 9, will still be significant in the coming decades. Therefore, it is crucial to consider SH SSWs as an influential factor in extreme weather forecasting for these regions in the near future.

Data availability. ERA5 data (Hersbach et al., 2020) is available via the Copernicus Climate Data Store (https://cds.climate.copernicus.eu). The model data used in this manuscript is published (Bischof et al., 2025) and available via https://zenodo.org/doi/10.5281/zenodo.16876611.

Author contributions. This study is partly based on the Bachelor Thesis by PR (née Garden) (Garden, 2022); SB wrote the manuscript and contributed substantially to the methodology design, data analysis and figure refinements; PR did large parts of the analysis and figures; RPK initiated the study, designed the methodology and guided its development; WH contributed to the design of the methodology; SW, RPK and SB designed and ran the model simulations; all authors contributed with discussions and feedback on the paper draft.

Competing interests. The authors declare that no competing interests are present.

Acknowledgements. This study was mainly funded by the GEOMAR Helmholtz Centre for Ocean Research in Kiel. Part of the funding for SB and RPK was granted through the 'Drivers of Jet stream anomalies' project of the Helmholtz Initiative on Climate Adaptation and Mitigation (HI-CAM) under the grant number RA-285/19. The model simulations were performed with resources provided by the North-German Supercomputing Alliance (HLRN), project shk00018.

References

Baldwin, M. P. and Dunkerton, T. J.: Stratospheric harbingers of anomalous weather regimes, Science (New York, N.Y.), 294, 581–4, https://doi.org/10.1126/science.1063315, 2001.

Baldwin, M. P., Ayarzagüena, B., Birner, T., Butchart, N., Butler, A. H., Charlton-Perez, A. J., Domeisen, D. I. V., Garfinkel, C. I., Garny, H., Gerber, E. P., Hegglin, M. I., Langematz, U., and Pedatella, N. M.: Sudden Stratospheric Warmings, Reviews of Geophysics, 59, 1–37, https://doi.org/10.1029/2020RG000708, 2021.

Bischof, S., Pilch Kedzierski, R., and Wahl, S.: Bischof et al. 2025 - southern hemisphere sudden stratospheric warmings continue to be relevant under global warming, https://doi.org/10.5281/ZENODO.16876611, tex.howpublished: [Data set] tex.year+duplicate-1: 2025, 2025.

Brovkin, V., Raddatz, T., Reick, C. H., Claussen, M., and Gayler, V.: Global biogeophysical interactions between forest and climate, Geophysical Research Letters, 36, 1–5, https://doi.org/10.1029/2009GL037543, 2009.

Butler, A. H., Seidel, D. J., Hardiman, S. C., Butchart, N., Birner, T., and Match, A.: Defining Sudden Stratospheric Warmings, Bulletin of the American Meteorological Society, 96, 1913–1928, https://doi.org/10.1175/BAMS-D-13-00173.1, iSBN: 6038621628, 2015.

Butler, A. H., Sjoberg, J. P., Seidel, D. J., and Rosenlof, K. H.: A sudden stratospheric warming compendium, Earth System Science Data, 9, 63–76, https://doi.org/10.5194/essd-9-63-2017, 2017.

Charlton, A. J. and Polvani, L. M.: A New Look at Stratospheric Sudden Warmings. Part I: Climatology and Modeling Benchmarks, Journal of Climate, 20, 449–469, https://doi.org/10.1175/JCLI3996.1, 2007.

Charlton, A. J., O'Neill, A., Lahoz, W. A., Massacand, A. C., and Berrisford, P.: The impact of the stratosphere on the troposphere during the southern hemisphere stratospheric sudden warming, September 2002, Quarterly Journal of the Royal Meteorological Society, 131, 2171–2188, https://doi.org/10.1256/qj.04.43, 2005.

Charney, J. G. and Drazin, P. G.: Propagation of planetary-scale disturbances from the lower into the upper atmosphere, Journal of Geophysical Research, 66, 83–109, https://doi.org/10.1029/JZ066i001p00083, 1961.

Chipperfield, M. P., Santee, M. L., Alexander, S. P., de Laat, A. T. J., Kinnison, D. E., Kuttippurath, J., Langematz, U., and Wargan, K.: Polar stratospheric ozone: Past, present, and future, in: Scientific assessment of ozone depletion: 2022, GAW report, p. 509, World Meteorological Organization, Geneva, Switzerland, https://csl.noaa.gov/assessments/ozone/2022/downloads/Chapter4_2022OzoneAssessment.pdf, number: 278 Section: 4, 2022.

Dennison, F. W., McDonald, A. J., and Morgenstern, O.: The effect of ozone depletion on the Southern Annular Mode and stratosphere-troposphere coupling, Journal of Geophysical Research Atmospheres, 120, 1–8, https://doi.org/10.1002/2014JD023009, 2015.

Eyring, V., Cionni, I., Bodeker, G. E., Charlton-Perez, A. J., Kinnison, D. E., Scinocca, J. F., Waugh, D. W., Akiyoshi, H., Bekki, S., Chipperfield, M. P., Dameris, M., Dhomse, S., Frith, S. M., Garny, H., Gettelman, A., Kubin, A., Langematz, U., Mancini, E., Marchand, M., Nakamura, T., Oman, L. D., Pawson, S., Pitari, G., Plummer, D. a., Rozanov, E., Shepherd, T. G., Shibata, K., Tian, W., Braesicke, P., Hardiman, S. C., Lamarque, J. F., Morgenstern, O., Pyle, J. A., Smale, D., and Yamashita, Y.: Multi-model assessment of stratospheric ozone return dates and ozone recovery in CCMVal-2 models, Atmospheric Chemistry and Physics, 10, 9451–9472, https://doi.org/10.5194/acp-10-9451-2010, 2010.

Feng, K., Rao, J., Garfinkel, C. I., Butler, A. H., Jie, W., Wu, T., Hitchcock, P., Lim, E.-P., Dowdy, A. J., and Seviour, W.: Can stratospheric nudging improve surface predictability? Insights from the 2019 Southern Hemisphere sudden stratospheric warming, npj Climate and Atmospheric Science, 8, 353, https://doi.org/10.1038/s41612-025-01234-2, 2025.

Garden, P. U.: Southern hemisphere sudden stratospheric warmings in the ECHAM6 model, Bachelor Thesis, CAU Kiel, 2022.

Gillett, N. P. and Thompson, D. W. J.: Simulation of Recent Southern Hemisphere Climate Change, Science, 302, 273–275, https://doi.org/10.1126/science.1087440, iSBN: 1094-4281, 2003.

Gillett, N. P., Kell, T. D., and Jones, P. D.: Regional climate impacts of the Southern Annular Mode, Geophysical Research Letters, 33, L23 704, https://doi.org/10.1029/2006GL027721, 2006.

Haase, S., Fricke, J., Kruschke, T., Wahl, S., and Matthes, K.: Sensitivity of the Southern Hemisphere circumpolar jet response to Antarctic ozone depletion: prescribed versus interactive chemistry, Atmospheric Chemistry and Physics, 20, 14 043–14 061, https://doi.org/10.5194/acp-20-14043-2020, 2020.

Hawkins, E. and Sutton, R.: The Potential to Narrow Uncertainty in Regional Climate Predictions, Bulletin of the American Meteorological Society, 90, 1095–1108, https://doi.org/10.1175/2009BAMS2607.1, 2009.

Hendon, H. H., Lim, E. P., and Abhik, S.: Impact of Interannual Ozone Variations on the Downward Coupling of the 2002 Southern Hemisphere Stratospheric Warming, Journal of Geophysical Research: Atmospheres, 125, 1–16, https://doi.org/10.1029/2020JD032952, 2020.

Hersbach, H., Bell, B., Berrisford, P., Hirahara, S., Horányi, A., Muñoz-Sabater, J., Nicolas, J., Peubey, C., Radu, R., Schepers, D., Simmons, A., Soci, C., Abdalla, S., Abellan, X., Balsamo, G., Bechtold, P., Biavati, G., Bidlot, J., Bonavita, M., De Chiara, G., Dahlgren, P., Dee, D., Diamantakis, M., Dragani, R., Flemming, J., Forbes, R., Fuentes, M., Geer, A., Haimberger, L., Healy, S., Hogan, R. J., Hólm, E., Janisková, M., Keeley, S., Laloyaux, P., Lopez, P., Lupu, C., Radnoti, G., de Rosnay, P., Rozum, I., Vamborg, F., Villaume, S., and Thépaut, J. N.: The ERA5 global reanalysis, Quarterly Journal of the Royal Meteorological Society, 146, 1999–2049, https://doi.org/10.1002/qj.3803, 2020.

Hirota, I., Kuroi, K., and Shiotani, M.: Midwinter warmings in the southern hemisphere stratosphere in 1988, Quarterly Journal of the Royal Meteorological Society, 116, 929–941, https://doi.org/10.1002/qj.49711649407, 1990.

Intergovernmental Panel on Climate Change (IPCC): Climate Change 2021 – The Physical Science Basis: Working Group I Contribution to the Sixth Assessment Report of the Intergovernmental Panel on Climate Change, Cambridge University Press, Cambridge, United Kingdom and New York, NY, USA, ISBN 978-1-009-15789-6, https://doi.org/10.1017/9781009157896, publication Title: Intergovernmental Panel on Climate Change (IPCC)_2023, 2023.

Ivanciu, I., Matthes, K., Wahl, S., Harlaß, J., and Biastoch, A.: Effects of prescribed CMIP6 ozone on simulating the Southern Hemisphere atmospheric circulation response to ozone depletion, Atmospheric Chemistry and Physics, 21, 5777–5806, https://doi.org/10.5194/acp-21-5777-2021, 2021.

Ivanciu, I., Matthes, K., Biastoch, A., Wahl, S., and Harlaß, J.: Twenty-first-century Southern Hemisphere impacts of ozone recovery and climate change from the stratosphere to the ocean, Weather and Climate Dynamics, 3, 139–171, https://doi.org/10.5194/wcd-3-139-2022, 2022a.

Ivanciu, I., Ndarana, T., Matthes, K., and Wahl, S.: On the Ridging of the South Atlantic Anticyclone Over South Africa: The Impact of Rossby Wave Breaking and of Climate Change, Geophysical Research Letters, 49, https://doi.org/10.1029/2022GL099607, 2022b.

Jucker, M., Reichler, T., and Waugh, D. W.: How Frequent Are Antarctic Sudden Stratospheric Warmings in Present and Future Climate?, Geophysical Research Letters, 48, 1–9, https://doi.org/10.1029/2021GL093215, 2021.

Kanzawa, H. and Kawaguchi, S.: Large stratospheric sudden warming in Antarctic late winter and shallow ozone hole in 1988, Geophysical Research Letters, 17, 77–80, https://doi.org/10.1029/GL017i001p00077, 1990.

Karpechko, A. Y., Hitchcock, P., Peters, D. H. W., and Schneidereit, A.: Predictability of downward propagation of major sudden stratospheric warmings, Quarterly Journal of the Royal Meteorological Society, 143, 1459–1470, https://doi.org/10.1002/qj.3017, iSBN: 9781424421770, 2017.

Krüger, K., Naujokat, B., and Labitzke, K.: The Unusual Midwinter Warming in the Southern Hemisphere Stratosphere 2002: A Comparison to Northern Hemisphere Phenomena, Journal of the Atmospheric Sciences, 62, 603–613, https://doi.org/10.1175/JAS-3316.1, iSBN: 0-408-70652-X, 2005.

Kwon, H., Choi, H., Kim, B.-M., Kim, S.-W., and Kim, S.-J.: Recent weakening of the southern stratospheric polar vortex and its impact on the surface climate over Antarctica, Environmental Research Letters, 15, 094 072, https://doi.org/10.1088/1748-9326/ab9d3d, 2020.

Labitzke, K.: Interannual Variability of the Winter Stratosphere in the Northern Hemisphere, Monthly Weather Review, 105, 762–770, https://doi.org/10.1175/1520-0493(1977)105<0762:IVOTWS>2.0.CO;2, 1977.

Labitzke, K.: Stratospheric-mesospheric midwinter disturbances: A summary of observed characteristics, Journal of Geophysical Research: Oceans, 86, 9665–9678, https://doi.org/10.1029/JC086iC10p09665, 1981.

Lim, E. P., Hendon, H. H., Boschat, G., Hudson, D., Thompson, D. W., Dowdy, A. J., and Arblaster, J. M.: Australian hot and dry extremes induced by weakenings of the stratospheric polar vortex, Nature Geoscience, 12, 896–901, https://doi.org/10.1038/s41561-019-0456-x, 2019.

Lim, E.-P., Hendon, H. H., Butler, A. H., Garreaud, R. D., Polichtchouk, I., Shepherd, T. G., Scaife, A., Comer, R., Coy, L., Newman, P. A., Thompson, D. W. J., and Nakamura, H.: The 2019 Antarctic sudden stratospheric warming, SPARC newsletter, pp. 10–undefined, 2020.

Lim, E. P., Hendon, H. H., Butler, A. H., Thompson, D. W., Lawrence, Z. D., Scaife, A. A., Shepherd, T. G., Polichtchouk, I., Nakamura, H., Kobayashi, C., Comer, R., Coy, L., Dowdy, A., Garreaud, R. D., Newman, P. A., and Wang, G.: The 2019 southern hemisphere stratospheric polar vortex weakening and its impacts, Bulletin of the American Meteorological Society, 102, E1150–E1171, https://doi.org/10.1175/BAMS-D-20-0112.1, 2021.

Lim, E.-P. P., Hendon, H. H., and Thompson, D. W. J.: Seasonal Evolution of Stratosphere-Troposphere Coupling in the Southern Hemisphere and Implications for the Predictability of Surface Climate, Journal of Geophysical Research: Atmospheres, 123, 12,002–12,016, https://doi.org/10.1029/2018JD029321, 2018.

Matthes, K., Biastoch, A., Wahl, S., Harlaß, J., Martin, T., Brücher, T., Drews, A., Ehlert, D., Getzlaff, K., Krüger, F., Rath, W., Scheinert, M., Schwarzkopf, F. U., Bayr, T., Schmidt, H., and Park, W.: The Flexible Ocean and Climate Infrastructure version 1 (FOCI1): mean state and variability, Geoscientific Model Development, 13, 2533–2568, https://doi.org/10.5194/gmd-13-2533-2020, 2020.

McLandress, C., Jonsson, A. I., Plummer, D. A., Reader, M. C., Scinocca, J. F., and Shepherd, T. G.: Separating the Dynamical Effects of Climate Change and Ozone Depletion. Part I: Southern Hemisphere Stratosphere, Journal of Climate, 23, 5002–5020, https://doi.org/10.1175/2010JCLI3586.1, iSBN: 0894-8755, 2010.

Meinshausen, M., Nicholls, Z. R., Lewis, J., Gidden, M. J., Vogel, E., Freund, M., Beyerle, U., Gessner, C., Nauels, A., Bauer, N., Canadell, J. G., Daniel, J. S., John, A., Krummel, P. B., Luderer, G., Meinshausen, N., Montzka, S. A., Rayner, P. J., Reimann, S., Smith, S. J., Van Den Berg, M., Velders, G. J., Vollmer, M. K., and Wang, R. H.: The shared socio-economic pathway (SSP) greenhouse gas concentrations and their extensions to 2500, Geoscientific Model Development, 13, 3571–3605, https://doi.org/10.5194/gmd-13-3571-2020, 2020.

Monge-Sanz, B. M., Bozzo, A., Byrne, N., Chipperfield, M. P., Diamantakis, M., Flemming, J., Gray, L. J., Hogan, R. J., Jones, L., Magnusson, L., Polichtchouk, I., Shepherd, T. G., Wedi, N., and Weisheimer, A.: A stratospheric prognostic ozone for seamless Earth system models: performance, impacts and future, Atmospheric Chemistry and Physics, 22, 4277–4302, https://doi.org/10.5194/acp-22-4277-2022, 2022.

Morgenstern, O., Zeng, G., Dean, S. M., Joshi, M., Abraham, N. L., and Osprey, A.: Direct and ozone-mediated forcing of the Southern Annular Mode by greenhouse gases, Geophysical Research Letters, 41, 9050–9057, https://doi.org/10.1002/2014GL062140, 2014.

Müller, W., Borchert, L., and Ghosh, R.: Observed Sub-Decadal Variations of European Summer Temperatures, Geophysical Research Letters, p. 2019GL086043, https://doi.org/10.1029/2019GL086043, 2019.

Naujokat, B. and Roscoe, H. K.: Evidence against an Antarctic Stratospheric Vortex Split during the Periods of Pre-IGY Temperature Measurements, Journal of the Atmospheric Sciences, 62, 885–889, https://doi.org/10.1175/JAS-3317.1, 2005.

Nordström, V. J. and Seppälä, A.: Does the coupling of the semiannual oscillation with the quasi-biennial oscillation provide predictability of Antarctic sudden stratospheric warmings?, Atmospheric Chemistry and Physics, 21, 12 835–12 853, https://doi.org/10.5194/acp-21-12835-2021, 2021.

Randel, W. J. and Wu, F.: Cooling of the Arctic and Antarctic polar stratospheres due to ozone depletion, Journal of Climate, 12, 1467–1479, https://doi.org/10.1175/1520-0442(1999)012<1467:COTAAA>2.0.CO;2, iSBN: 0894-8755, 1999.

Rao, J., Garfinkel, C. I., White, I. P., and Schwartz, C.: The Southern Hemisphere Minor Sudden Stratospheric Warming in September 2019 and its Predictions in S2S Models, Journal of Geophysical Research: Atmospheres, 125, 1–19, https://doi.org/10.1029/2020JD032723, 2020.

Rao, J., Garfinkel, C. I., Wu, T., Lu, Y., and Chu, M.: Mean State of the Northern Hemisphere Stratospheric Polar Vortex in Three Generations of CMIP Models, Journal of Climate, 35, 4603–4625, https://doi.org/10.1175/JCLI-D-21-0694.1, 2022.

Reick, C. H., Raddatz, T., Brovkin, V., and Gayler, V.: Representation of natural and anthropogenic land cover change in MPI-ESM, Journal of Advances in Modeling Earth Systems, 5, 459–482, https://doi.org/10.1002/jame.20022, 2013.

Revell, L. E., Robertson, F., Douglas, H., Morgenstern, O., and Frame, D.: Influence of Ozone Forcing on 21st Century Southern Hemisphere Surface Westerlies in CMIP6 Models, Geophysical Research Letters, 49, 1–9, https://doi.org/10.1029/2022GL098252, 2022.

Rind, D., Suozzo, R., Balachandran, N. K., and Prather, M. J.: Climate Change and the Middle Atmosphere. Part I: The Doubled CO2 Climate, Journal of the Atmospheric Sciences, 47, 475–494, https://doi.org/10.1175/1520-0469(1990)047<0475:CCATMA>2.0.CO;2, 1990.

Safieddine, S., Bouillon, M., Paracho, A. C., Jumelet, J., Tencé, F., Pazmino, A., Goutail, F., Wespes, C., Bekki, S., Boynard, A., Hadji-Lazaro, J., Coheur, P. F., Hurtmans, D., and Clerbaux, C.: Antarctic Ozone Enhancement During the 2019 Sudden Stratospheric Warming Event, Geophysical Research Letters, 47, 1–10, https://doi.org/10.1029/2020GL087810, 2020.

Scherhag, R.: Die explosionsartige Stratosphären-Erwärmung des Spätwinters 1951/52, Berichte des DWD in der US-Zone, 6, 1952.

Schoeberl, M. R., Stolarski, R. S., and Krueger, A. J.: The 1988 Antarctic ozone depletion: Comparison with previous year depletions, Geophysical Research Letters, 16, 377–380, https://doi.org/10.1029/GL016i005p00377, 1989.

Shiotani, M. and Hirota, I.: Planetary wave-mean flow interaction in the stratosphere: A comparison between northern and southern hemispheres, Quarterly Journal of the Royal Meteorological Society, 111, 309–334, https://doi.org/10.1002/qj.49711146804, 1985.

Sigmond, M., Scinocca, J. F., Kharin, V. V., and Shepherd, T. G.: Enhanced seasonal forecast skill following stratospheric sudden warmings, Nature Geoscience, 6, 98–102, https://doi.org/10.1038/ngeo1698, 2013.

Solomon, S., Ivy, D. J., Kinnison, D., Mills, M. J., Neely, R. R., and Schmidt, A.: Emergence of healing in the Antarctic ozone layer, Science, 353, 269–274, https://doi.org/10.1126/science.aae0061, arXiv: 1512.04598 ISBN: 1095-9203 (Electronic) 0036-8075 (Linking), 2016.

Stolarski, R. S., McPeters, R. D., and Newman, P. A.: The Ozone Hole of 2002 as Measured by TOMS, Journal of the Atmospheric Sciences, 62, 716–720, https://doi.org/10.1175/JAS-3338.1, 2005.

Thompson, D. W. J. and Solomon, S.: Interpretation of Recent Southern Hemisphere Climate Change, Science, 296, 895–899, https://doi.org/10.1126/science.1069270, iSBN: 0036-8075, 2002.

Thompson, D. W. J. and Solomon, S.: Recent stratospheric climate trends as evidenced in radiosonde data: Global structure and tropospheric linkages, Journal of Climate, 18, 4785–4795, http://scholar.google.com/scholar?hl=en&btnG=Search&q=intitle:Recent+Stratospheric+Climate+Trends+as+Evidenced+in+Radiosonde+Data+:+Global+Structure+and+Tropospheric+Linkages#0, 2005.

Thompson, D. W. J. and Wallace, J. M.: Annular Modes in the Extratropical Circulation. Part I: Month-to-Month Variability*, Journal of Climate, 13, 1000–1016, http://scholar.google.com/scholar?hl=en&btnG=Search&q=intitle:Annular+Modes+in+the+Extratropical+Circulation+.+Part+I+:+Month-to-Month+Variability+*#0, 2000.

Thompson, D. W. J., Baldwin, M. P., and Solomon, S.: Stratosphere–Troposphere Coupling in the Southern Hemisphere, Journal of the Atmospheric Sciences, 62, 708–715, https://doi.org/10.1175/JAS-3321.1, 2005.

Thompson, D. W. J., Solomon, S., Kushner, P. J., England, M. H., Grise, K. M., and Karoly, D. J.: Signatures of the Antarctic ozone hole in Southern Hemisphere surface climate change, Nature Geoscience, 4, 741–749, https://doi.org/10.1038/ngeo1296, 2011.

Wang, L., Hardiman, S. C., Bett, P. E., Comer, R. E., Kent, C., and Scaife, A. A.: What chance of a sudden stratospheric warming in the southern hemisphere?, Environmental Research Letters, 15, https://doi.org/10.1088/1748-9326/aba8c1, 2020.

Wargan, K., Weir, B., Manney, G. L., Cohn, S. E., and Livesey, N. J.: The Anomalous 2019 Antarctic Ozone Hole in the GEOS Constituent Data Assimilation System With MLS Observations, Journal of Geophysical Research: Atmospheres, 125, 1–28, https://doi.org/10.1029/2020JD033335, 2020.

Wu, Z. and Reichler, T.: Variations in the Frequency of Stratospheric Sudden Warmings in CMIP5 and CMIP6 and Possible Causes, Journal of Climate, 33, 10 305–10 320, https://doi.org/10.1175/JCLI-D-20-0104.1, 2020.

Xu, X., Martin, T., Beadling, R. L., Liu, J., Bischof, S., Hattermann, T., Huo, W., Li, Q., Marshall, J. C., Muilwijk, M., Pauling, A. G., Purich, A., Smith, I. J., Swart, N. C., and Thomas, M.: Robustness and Mechanisms of the Atmospheric Response Over the Southern Ocean to Idealized Freshwater Input Around Antarctica, Geophysical Research Letters, 52, e2024GL113 734, https://doi.org/10.1029/2024GL113734, 2025.

Zheng, F., Li, J., and Liu, T.: Some advances in studies of the climatic impacts of the Southern Hemisphere annular mode, Journal of Meteorological Research, 28, 820–835, https://doi.org/10.1007/s13351-014-4079-2, arXiv: 1011.1669 Place: Cambridge ISBN: 9788578110796, 2014.

Zi, Y., Long, Z., Sheng, J., Lu, G., Perrie, W., and Xiao, Z.: The Sudden Stratospheric Warming Events in the Antarctic in 2024, Geophysical Research Letters, 52, https://doi.org/10.1029/2025gl115257, 2025.